P- ISSN 1991-8941 E-ISSN 2706-6703
2021,15 (2):60 – 65

Journal of University of Anbar for Pure Science (JUAPS)

Open Access

Novel Ester Monomers and Its Transition Metal Polychelates and Their Photovoltaic Application On Dye Sensitized Solar Cells

Sadeem M. Al-Barody*
Department of Chemistry, College of Science, University of Al-Mustansiriyah, Baghdad, Iraq

ARTICLE INFO

Received: 7 / 11 /2021
Accepted: 28 / 11 / 2021
Available online: 21/ 12 / 2021

DOI:
http://dx.doi.org/10.37652/JUAPS.2021.15.2.9

Keywords:
Schiff base,
Transition metals,
Dye-Sensitized Solar Cell,
Photovoltaic Performance,

ABSTRACT

A novel ligand N-(2-hydroxyl phenyl)-(4′-pentloxy-benzate-salicyIidene) (H_2L) prepared by 1:1 molar ratio of 4-pentyloxy (4′-formyl-3′-hydroxy)-benzoate and 2-aminophenol, synthesis of [$M(H_2L)H_2O$] and [Cu_2L_2] complexes were described by IR spectroscopy, C.H.N.O, ^1H, $^{13}CNMR$, , GCmass. photovoltaic measurement of H_2L and Cu_2L_2 as photosensitizers by dye-sensitized solar cells (DSSCs) the best result was for Cu_2L_2 than H_2L.

1. INTRODUCTION

The unique physical and chemical properties of liquid crystals gave them very important attention [1]. Because of their ability to make complexes with a wide range of metals, more than 30 years of study were focused on LCD research [2-4]. 11.1% energy efficiency was the highest result of DSSCs [5]. Our laboratory published many papers in the field of liquid crystals [6–9]. We report this work as a continuation of our research. A novel mesogenic (smectic), ligand N-(2-hydroxyl phenyl)-(4′-pentloxy-benzate-salicyIidene) (H_2L) prepared by 1:1 molar ratio of 4-pentyloxy (4′-formyl-3′-hydroxy)-benzoate and 2-aminophenol, synthesis of [$M(H_2L)H_2O$] and [Cu_2L_2] complexes were described by IR spectroscopy, C.H.N.O, ^1H, $^{13}CNMR$, , GCmass . In addition, their performance in dye-sensitized solar cells has been studied.

METHODOLOGY:

The analytical grade was used for all chemicals. The experiment and the measurements were done at, UPM, Faculty of Science, Malaysia.

(1) 4-Pentyloxybenzoic Acid:

Solution of 150 mL ethanol with 11.05 g of hydroxybenzoic acid 80 mm0l and 50 mL ethanol with 8.97 g KOH 160 mm0l, dropwise addition of 10 mL of 1-bromopentane 80 mm0l. The reaction mixture was refluxed for ~14 h under a dry atmosphere and allowed to come to room temperature.

The solid alkoxy potassium salt obtained was separated out by filtration under suction and treated with dilute HCl until the pH of the reaction mixture reached ~2 h. The crude solid white product was filtered off, washed thoroughly with water, and recrystallized successively from solutions of glacial acetic acid and toluene [10]. Yield: (75%) Scheme 1. shows synthesis details.

(2) 4-Pentyloxy (4′-Formyl-3′-Hydroxy)-Benzoate:

10.40 g 4-pentyloxybenzoic 50 mmol and 6.90 g 2,4 dihydroxybenzaldehyde 50 mmol in 100 mL chloroform with DCC with 0.3 g catalyst like DMAP stirred for ~12 h at room temperature. White solid ester 2 was formed [10]. Yield: (65%).

(3)N-(2-hydroxylphenyl)-(4′-pentyloxybenzoate-salicylidene) (H_2L):

Absolute ethanolic solutions of (20 mmol, 6.56 g in 100 mL) 4-pentyloxy-(4′-formyl-3′-hydroxy)benzoate and (20 mmol, 5.64 g in 20 mL) 2-aminophenol were refluxed for ~4 h in presence of a few drops of acetic acid and the resultant solution was left over-night in the reaction flask at room temperature. The micro-crystalline pale yellow product, 3, was suction-filtered, thoroughly washed with ethanol, recrystallized from a solution of absolute ethanol/chloroform (v/v, 1/1), and dried at room temperature. Yield: (60%); m.p., 85℃.

Synthesis of the Complexes:

* Corresponding author at Department of Chemistry, College of Science, University of Al-Mustansiriyah
Corresponding author. E-mail: sadeemaaa@yahoo.com

Dissolved metal salts were M= Co, Mn, Zn, Ni, and Cu ($MCl_2.XH_2O$) in 25 ml ethanol to 0.42 g (H_2L) in 50 mL ethanol. cold ethanol was washed the precipitated.

Assembling the DSSCs:

The cell looks like a sandwich-type; one side was ITO carbon counter electrode, then a solution of 0.05 M I_2 and 0.5 M KI were inserted between the two layers. To illuminate the cell, we used sunlight for DSSCs. Open-circuit and short circuit Photo voltage were measured by (Keithley 2400). The equation below gives the power conversion efficiency η [11]:

$$\eta = \frac{I_{sc} V_{oc} FF}{P_{in}} \qquad (1)$$

In (1), V_{oc} is the voltage of open-circuit, I_{sc} is the photocurrent of short-circuit, P_{in} light power, The fill factor FF is determined by [12]:

$$FF = \frac{V_m I_m}{V_{oc} I_{sc}} \qquad (2)$$

In (2), V_{max} voltage and I_{max} current represent the maximum respectively.

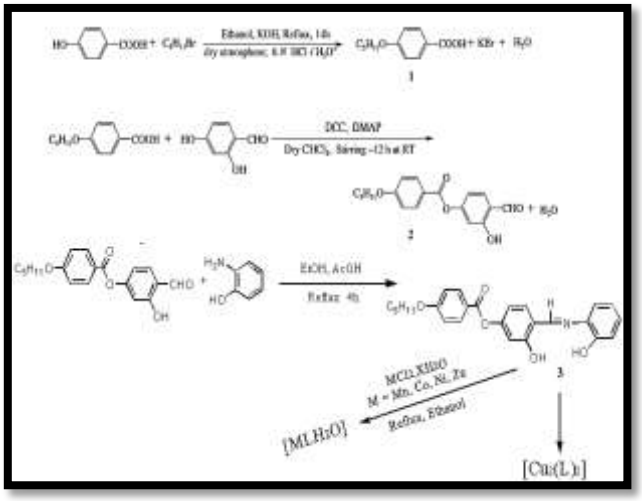

Scheme1: H_2L and its complexes pathway.

RESULTS AND DISCUSSION:

Mononuclear complexes (complexes 1 – 4) were formed by the complexation of H_2L with M= Co Cu Ni Mn and Zn, complex (5) shows dinuclear. All were stable, colored, DMF soluble. [13]. All the physical properties are in (Table 1).

FT- IR SPECTRA:

H_2L IR chart show two bands at 3660, 3250 cm^{-1} refer to ν [OH1, OH2] phenolic respectively. The band shows broadness because of the N=C ⋯ OH [4]. 1730 cm^{-1} for ν(C=O) and 1145 cm^{-1} for ν(C–O) [14-15]. coordinated water in all complexes have absorption at 3292 cm^{-1} to ν(OH) [11], [16]. thermogravimetric give more evidence for the presence of water molecule. During the coordination, The shifted from (1607 to 1595 cm^{-1}) for ν(C=N) a good proof that electrons withdraw from the N azomethine atom to the M metal [4]. The participation of phenolic oxygen in coordination is proof by the change of C-O stretching from 1153-1135 cm^{-1} in H_2L to 1171–1140 cm^{-1} of the complexes [13], [14], [16]. More evidence about the azomethine N and phenolic O of the ligand to coordinate with the M ion are listed in (Table 2) [15].

Table 1: physical properties of H_2L and its complexes as well as Elemental analysis.

sample	M.wt	C	H	N	O	Molar conductivity
H_2L $C_{25}H_{25}NO_5$	419	72.597 1.45	5.96 5.90	3.34 3.30	19.09 19.19	--
$C_{25}H_{25}NO_6Mn$	489	61.24 61.45	5.10 5.15	2.86 2.95	19.601 9.68	2.2
$C_{25}H_{25}NO_6Co$	493	60.74 60.88	5.06 5.10	2.84 2.84	19.44 19.40	2.4
$C_{25}H_{25}NO_6Ni$	493	60.72 60.79	5.06 5.12	2.83 2.76	19.43 19.50	1.1
$C_{25}H_{25}NO_6Zn$	500	60.00 60.20	5.00 5.08	2.80 2.81	19.20 19.29	0.0
$C_{50}H_{46}N_2O_{10}Cu_2$	961	62.34 62.45	4.78 4.85	2.91 2.85	16.64 16.67	1.3

Table 2: IR bands of H_2L and its complexes (cm^{-1}).

SAMPLE	ν(OH)	ν(C=N)	ν(M-O)	ν(M-N)
H_2L ($C_{25}H_{25}NO_5$)	**3659-3250**	**1607**	--	--
$C_{25}H_{25}NO_6Mn$	**3292**	**1595**	**492-430**	**583-513**
$C_{25}H_{25}NO_6Co$	**3290**	**1595**	**490-431**	**583-513**
$C_{25}H_{25}NO_6Ni$	**3292**	**1595**	**492-430**	**583-513**
$C_{25}H_{25}NO_6Zn$	**3288**	**1590**	**494-433**	**583-514**
$C_{50}H_{46}N_2O_{10}Cu_2$]	------	**1580**	**496-433**	**583-513**

^{1}HNMR SPECTRA:

DMSO used as solvent for all ^{1}HNMR spectra and TMS as standard. (Figure 2) shows δ 13.96 ppm for $OH_{1"}$ and for $OH_{2"}$ at δ 10.02 ppm at δ 8.49 ppm Singlet signal for CH=N [5]. aromatic protons appear as Multiples signals at δ 7.9 -7.3 ppm, at δ 3.9 - 0.8 ppm of H_{23},H_{22},H_{21},H_{20},H_{19}. ^{1}HNMR (500 MHz, DMSO) δ ppm: 14.92 (s, 1H, $H_{1"}$) ppm, 10.01 (s, 1H, $H_{2"}$), 9.13 (d, 2H, $H_{6,2}$), 7.78 (m, 4H, $H_{17,15,16,14}$), 7.28 (d, 1H, H_9), 6.96 (d, 2H, $H_{3,5}$), 6.82 (d, 1H, H_{12}), 6.75 (dd, 1H, H_8), 4.07 (t, 2H, H_{19}), 1.85–1.40 (m, 6H, $H_{20,21,22}$), 0.96 (3H, H_{23}) [7-16] (Figure 1). ^{1}H NMR spectrum of Zn(II) complex diamagnetic (Figure 3) shows The absence of -OH signals in Zn(II) spectrum refer to hydroxyl deprotonation of the H_2L coordination with Zn(II), [17].

Moreover, the downfield region δ 8.21 ppm of the imine carbon proton good indication that an atom coordinates to Zn(II) [17], [18].

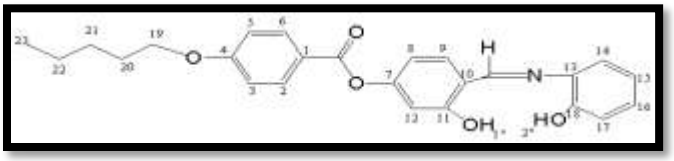

Fig. 1: NMR spectra of H2L.

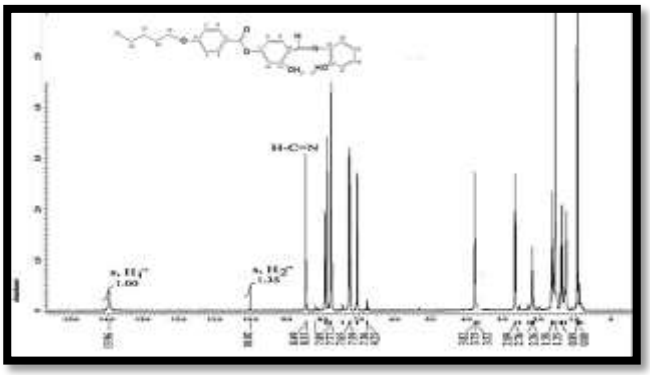

Fig. 2: H_2L ^{1}HNMR spectrum.

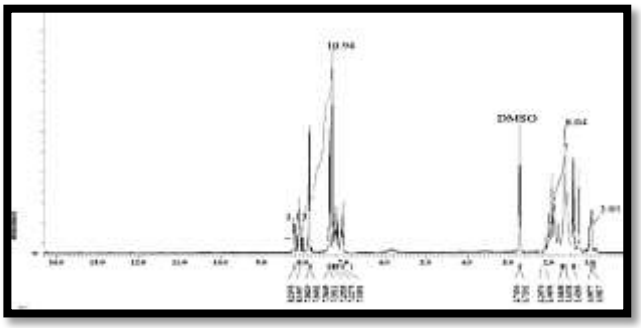

Fig. 3: $[ZnL(H_2O)]^1$HNMR spectrum.

ELECTRONIC TRANSITION AND MAGNETIC SUSCEPTIBILITY

Table 3 shows absorption bands and their assignment, intra ligand transitions at 35,621 π–π and 26,865 cm^{-1} n–π* [19]. All the previous transitions shifted to longer wavelengths in the complexes confirming the complexation. In Cu(II) complex the $2B_{1g} \rightarrow {}^2A_1g$ and $^2B_{1g} \rightarrow {}^2B_{2g}$ appear as broadband and shoulder at 18,275 and 17,122 cm^{-1} respectively related to square-planar [19]. Magnetic susceptibility (1.83 BM) suggested that no interaction between metal centers and give more evidence for square-planar geometry [20]. Two bands for Tetrahedral Ni(II) complex at 17,700 $^3T_1(F) \rightarrow {}^3T_1(P)$ and 14,880 $cm^{-1}{}^3T_1(F) \rightarrow {}^3A_2$ (F), [20]. The magnetic suitability (2.83 BM) 3.0–3.5 could be for distorted tetrahedral complexes [21]. 16,583 cm^{-1} to d–d band for square-planar Co(II) assigned to $^1A_{1g} \rightarrow {}^1B_{1g}$, magnetic susceptibility (3.85 BM) a proof this geometry. (LMCT) at 22,522 cm^{-1} in Mn(II) complex, [22]. Furthermore, the 5.21 BM indicated the tetrahedral structure. Finally, moderately band at 24,875 cm^{-1} in tetrahedral Zn(II) complex assigned to charge transfer [23].

Table 3: Characteristics UV-Vis. and magnetic suitability of H_2L and its complexes.

samples	UV-Vis (cm^{-1}, DMSO)	Assignments	$\mu_{eff.}$ (BM)
H_2L	35,621, 26,865	π–π n–π*	--
$MnL(H_2O)$	36,621, 27,865, 22.522	π–π n–π* CT	5.21
$CoL(H_2O)$	35,621, 26,865, 16,583	π–π n–π* $^1A_{1g} \rightarrow {}^1B_{1g}$	3.85
$NiL(H_2O)$	35,729, 27,735, 17,699, 14,880	π–π n–π* $^3T_1(F) \rightarrow {}^3T_1(P)$ $^3T_1(F) \rightarrow {}^3A_2$ (F)	2.83
$ZnL(H_2O)$	35,661, 26,876, 24,875	π–π n–π* CT	Dia.
Cu_2L_2	36,621, 27,865, 18,275, 17,122	π–π n–π* $^2B_{1g} \rightarrow {}^2A_1g$ $^2B_{1g} \rightarrow {}^2B_{2g}$	1.83

GC-MASS SPECTRA

(Figure 4) illustrated the GC-Mass of H_2L, mwt. of the H_2L ($C_{25}H_{25}NO_5$) matched with M+ peak at m/z = 419, [fragment, intensity %] 420 [M+1, 20], 419 [M, 25], 348 [M-C_5H_{11}, 35], 298 [M-$HOPhCO^+$, 30], 228 [M-$C_5H_{11}OPhCO$, 100], 402 [$C_5H_{11}OPhCOOPh(OH)CH=NPh^+$, 35], 326 [$C_5H_{11}OPhCOOPh(OH)CH=N^+$, 15] , 191 [$C_5H_{11}O$-Ph-$CO^+$, 40], 121 [$HOPhCO^+$, 20], 71 [$C_5H_{11}{}^+$, 10]. GC-Mass are given in (Table 4), (Figure 5) for GC-Mass of Cu(II) complex

Table 4: GC-mass data of the complexes.

samples	Molar mass	m/z values [fragment, intensity %]
$MnL(H_2O)$	460.17	442 [M−H_2O, 50], 263 [M−($C_{13}H_9N+H_2O)^+$, 60], 247 [M−($C_{13}H_9NO+H_2O)^+$, 70]
$CoL(H_2O)$	462.16	444 [M−H_2O, 45], 265 [M−($C_{13}H_9N+H_2O)^+$, 33], 249 [M−($C_{13}H_9NO+H_2O)^+$, 80]
$NiL(H_2O)$	463.16	445 [M−H_2O, 35], 266 [M−($C_{13}H_9N+H_2O)^+$, 45], 250 [M−($C_{13}H_9NO+H_2O)^+$, 60]
$ZnL(H_2O)$	465.22	447 [M−H_2O, 55], 268 [M−($C_{13}H_9N+H_2O)^+$, 55], 252 [M−($C_{13}H_9NO+H_2O)^+$, 65]
Cu_2L_2	962.12	767 [M−($C_{13}H_9NO)^+$, 40] , 783 [M−($C_{13}H_9N)^+$, 40], 820 [M−2(C_5H_{11})$^+$, 30], 580 [M−2($C_5H_{11}O$-Ph-CO)$^+$, 35],548 [M−2($C_5H_{11}O$-Ph-COO)$^+$,15]

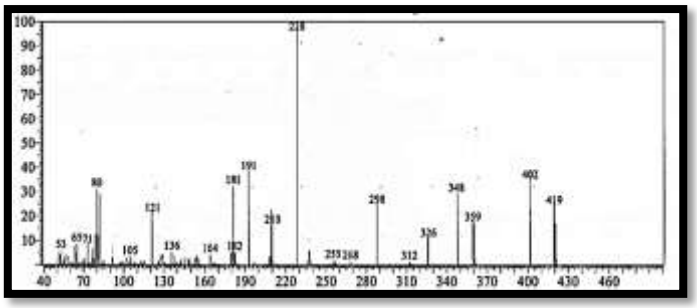

Fig. 4: H_2L Mass spectrum.

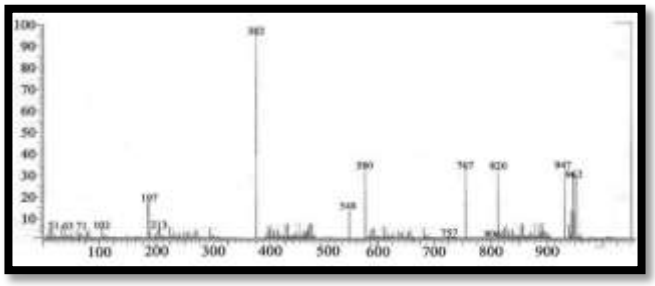

Fig. 5: [Cu_2L_2] Mass spectrum.

TGA CHARACTERIZATION OF H_2L AND ITS COMPLEXES

The temperature ranges from 10 − 1000 ℃ with a 10 °C min^{-1} heating rate and under nitrogen atmosphere, TGA analyses were carried for all complexes (Table 5). Ni(III) TG shows no loss of water below 362 ℃ (Figure 6) [24]. Between 178 - 403 ℃ temperature, 48.59 % first weight loss of the complexes was observed this loss was matched with [($C_5H_{11}O$-C_6H_6-COO) + H_20] and has been confirmed by (0.7143 mg) while loss of ($C_{13}H_9N$) as 42.11 % observed as (0.6191 mg) in the temperature range 408−498 ℃, after 498 °C mass loss, metal oxide which is thermally stable form.

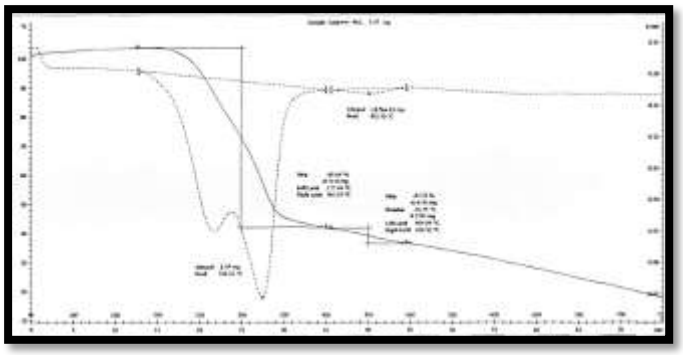

Fig. 6: TGA Curve of [NiL(H_2O)] complex.

Table 4: TGA characteristics of complexes.

Compounds	decomposition step ℃	% W. Loss observed. (calc.)	Eliminated species
($C_{25}H_{25}NO_6Mn$)	355-365	48.96 (48.91)	$C_5H_{11}0$-C_6H_6-C00 + H_20
	377-384	38.96 (38.91)	$C_{13}H_9N$
	470	18.93 (18.91)	$Mn0_2$ Residue
($C_{25}H_{25}NO_6Co$)	285-310	48.80 (48.70)	$C_5H_{11}0$-C_6H_6-C00 + H_20
	320-365	42.32 (42.20)	$C_{13}H_9N0$
	431	16.31 (16.23)	CoO Residue
($C_{25}H_{25}NO_6Ni$)	177-402	48.64 (48.59)	$C_5H_{11}0$-C_6H_6-C00 + H_20
	408-498	42.22 (42.11)	$C_{13}H_9N0$
	500	16.25 (16.19)	NiO Residue
[$C_{50}H_{46}N_2O_{10}Cu_2$]	320-379	43.25 (43.03)	2-($C_5H_{11}0$-C_6H_6-C00)
	385-395	40.60 (40.54)	2-($C_{13}H_9N$)
	400	16.75 (16.62)	CuO Residue

CURRENT-VOLTAGE MEASUREMENT OF DSSCS

Compounds with imine group can be represented as the hole can transport. To study this characterization, we need to study current-voltage properties [27]. (Figure 7) reported I-V curves under direct sunlight for both H_2L and Cu_2L_2 DSSCs. The current-density curve was the largest for Cu_2L_2 indicating that highest output power was generated by this cell. while, smallest current – density has been reported for H_2L DSSCs. So lower power can be generated. (Table 5) reported photovoltaic parameters. From data in table 5, we can notice that more electrons injected from Cu_2L_2 cell to TiO conductive bands

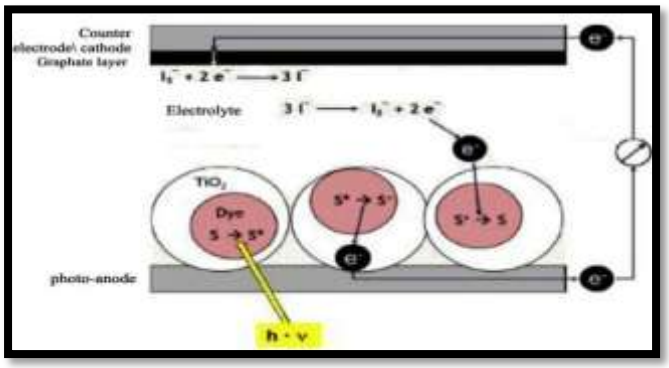

Fig. 7: current-voltage characteristics of ester dye-sensitized solar cell.

Isc: (mA.cm-2) Short circuit current; ; Im: (mA.cm^{-2}) Maximum current; Voc: (mV) Open circuit voltage Vm: η: (mV) overall energy conversion: Maximum voltage; FF: Fill factor; yield

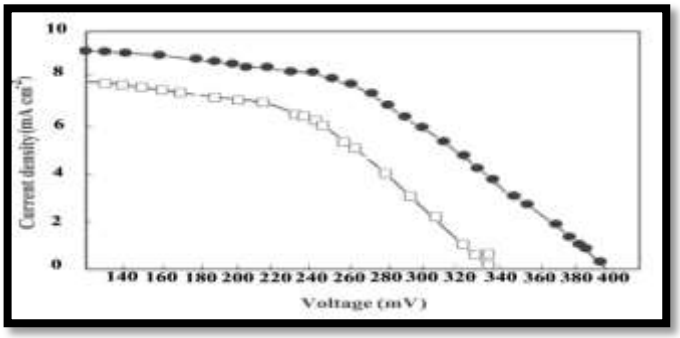

Fig. 8: Schematic of DSSC with a TiO_2-coated electrode [28].

Table 5: parameters of H_2A and H_2A-Cu Photovoltaic dyes sensitized solar cells.

Compound	I_{SC}	V_{OC}	I_m	V_m	FF	η×10^{-2} %
H_2L	7.85	343	7	228	0.55	1.59
Cu_2L_2	9.64	398	8	258	0.52	2.10

CONCLUSION

A novel ligand N-(2-hydroxyl phenyl)-(4′-pentloxy-benzate-salicylidene) (H_2L) prepared by 1:1 molar ratio of 4-pentyloxy (4′-frmyl-3′-hydrxy)-benzoate and 2-aminophen0l,

synthesis of $[M(H_2L)H_2O]$ and $[Cu_2L_2]$ complexes were described by IR spectroscopy, C.H.N.O, ^{1}H, $^{13}CNMR$, GC mass. square planar was proposed for Cu(II), Co(II) complexes, whereas Mn(II), Ni(II) and Zn(II) show tetrahedral. All complexes are thermally stable, highest short-circuit for Cu_2L_2 the density I_{SC} was 9.64 $mA.cm^{-2}$ and 2.10%. conversion efficiency

FUNDING

Big thanks to the University of Putra Malaysia for carrying out the physical measurements.

REFERENCES

[1] Mujtahid, F., Gareso, P. L., Armynah, B., & Tahir, D. (2021). Review effect of various types of dyes and structures in supporting performance of dye- sensitized solar cell TiO2- based nanocomposites. *International Journal of Energy Research*.

[2] Farhana, N. K., Saidi, N. M., Bashir, S., Ramesh, S., & Ramesh, K. (2021). Review on the Revolution of Polymer Electrolytes for Dye-Sensitized Solar Cells. *Energy & Fuels*.

[3] Bist, A., & Chatterjee, S. (2021). Review on Efficiency Enhancement Using Natural Extract Mediated Dye-Sensitized Solar Cell for Sustainable Photovoltaics. *Energy Technology*, *9*(8), 2001058..

[4] Almutairi, M. A., Farooq, W. A., & AlSalhi, M. S. (2021). Photovoltaic and impedance properties of dye-sensitized solar cell based on nature dye from beetroot. *Current Applied Physics*.

[5] Can, M., Havare, A. K., & Akan, E. (2021). Dye-Sensitized Solar Cell (DSSC) Applications based on Cyano Functional Small Molecules Dyes. *Int J Opt Photonic Eng*, *6*, 040. [6] Khalil A, Sadeem M, Haslina A. *Journal of Applied Chemistry* 2014; Vol. 2, pp 71-81.

[7] Khalil A., Sadeem M. *Liquid Crystals* 2014; pp1-12. doi: 10.1080/02678292.2014.919670

[8] Al-Barody, S. M. and H. Ahmad (2015). "Synthesis, structural characterization and thermal studies of lanthanide complexes with Schiff base ligand N, N′-di-(4′-pentyloxybenzoate)-salicylidene-1, 3-diaminopropane." Cogent Chemistry **1**(1): 1093920..

[9] Al-Barody, S. (2018). "Characterization and Thermal Study of Schiff-Base Monomers and Its Transition Metal Polychelates and Their Photovoltaic Performance on Dye Sensitized Solar Cells." Journal of Structural Chemistry **59**(1): 53-63

[10] Varga, Z., & Rácz, E. (2021, January). Influence of the Cell Temperature on the Performance of a Dye Sensitized Solar Cell. In *2021 IEEE 19th World Symposium on Applied Machine Intelligence and Informatics (SAMI)* (pp. 000175-000180). IEEE.

[11] Gao, N., Huang, L., Li, T., Song, J., Hu, H., Liu, Y., & Ramakrishna, S. (2020). Application of carbon dots in dye- sensitized solar cells: a review. *Journal of Applied Polymer Science*, *137*(10), 48443.

[12] Khan, M. I., Fatima, N., Mustafa, G. M., Sabir, M., Abubshait, S. A., Abubshait, H. A., ... & Baig, M. R. (2021). Improved photovoltaic properties of dye sensitized solar cell by irradiations of Ni2+ ions on Ag-doped TiO2 photoanode. *International Journal of Energy Research*, *45*(6), 9685-9693.

[13] Gao, S., Li, Q., Baryshnikov, G., Ågren, H., & Xie, Y. (2021). Synthesis, characterization, and spectroscopic properties of 2- (3, 5, 6- trichloro- 1, 4- benzoquinon-2- yl)- neo- fused hexaphyrin. *Bulletin of the Korean Chemical Society*.

[14] Singh, A., Dutta, A., Srivastava, D., Kociok- Köhn, G., Chauhan, R., Gosavi, S. W., ... & Muddassir, M. (2021). Effect of different aromatic groups on photovoltaic performance of 1, 1′- bis (diphenylphosphino) ferrocene functionalized Ni (II) dithiolates as sensitizers in dye sensitized solar cells. *Applied Organometallic Chemistry*, e6402.

[15] Watson, J., Santaloci, T. J., Cheema, H., Fortenberry, R. C., & Delcamp, J. H. (2020). Full Visible Spectrum Panchromatic Triple Donor Dye for Dye-Sensitized Solar Cells. *The Journal of Physical Chemistry C*, *124*(46), 25211-25220.

[16] Abdel A., Ayman A., Abdel Naby M. Salem, Mohamed M. " Synthesis, structural characterization, thermal studies, catalytic efficiency and antimicrobial activity of some M(II) complexes with ONO tridentate Schiff base N-salicylidene-o-aminophenol (saphH2)." *Journal of Molecular Structure* 1010 (2012): 130-138.

[17] A. Majumder, G.M. Rosair, A. Mallick, N. Chattopadhyay, S. Mitra, Polyhedron 25 (2006) 1753.

[18] M.S. El-Shahawi, A.F. Shoair, Spectrochim. Acta A 60 (2004) 121.

[19] A.B.P. Lever, Inorganic Electronic Spectroscopy, second ed., Elsevier Science,Amsterdam, 1984.

[20] N. Raman, S.J. Raja, J. Joseph, J.D. Raja, J. Chil. Chem. Soc. 52 (2007) 1138.

[21] A.A. Soliman, Spectrochim. Acta A 65 (2006) 1180.

[22] H. Asada, K. Hayashi, S. Negoro, M. Fujiwara, T. Matsushita, Inorg. Chem. Commun. 6 (2003) 193.

[23] L.A. Saghatforoush, A. Aminkhani, S. Ershad, G. Karimnezhad, S. Ghammamy, R. Kabiri, Molecules 13 (2008) 804.

[24] T. Katsuki, Coor. Chem. Rev. 140 (1995) 189.

[25] Vikraman, D., Hussain, S., Patil, S. A., Truong, L., Arbab, A. A., Jeong, S. H., ... & Kim, H. S. (2021). Engineering MoSe2/WS2 hybrids to replace the scarce platinum electrode for hydrogen evolution reactions and dye-sensitized solar cells. *ACS Applied Materials & Interfaces*, *13*(4), 5061-5072. [26] Sadeem M., Khalil A., *Lanthanides Liquid Crystaline of Azobenzene Schiff Base*. 2014: LAP Lambert Academic Publishing, 9783659519338.

[27] Shanmugapriya, T., & Balavijayalakshmi, J. (2021). Role of graphene oxide/yttrium oxide nanocomposites as a cathode material for natural dye- sensitized solar cell applications. *Asia- Pacific Journal of Chemical Engineering*, *16*(2), e2598.

[28] Maddala, G., Ambapuram, M., Tankasala, V., & Mitty, R. (2021). Optimal Dye Sensitized Solar Cell and Photocapacitor Performance with Efficient Electrocatalytic SWCNH Assisted Carbon Electrode. *ACS Applied Energy Materials*, *4*(10), 11225-11233.

مونيمرات الاستر ومعقداته مع العناصر الانتقالية وتطبيقاتهم الكهروضوئية كخلايا شمسية ذات صبغات متحسسة للضوء

سديم محمد البارودي

قسم الكيمياء ، كلية العلوم ، الجامعه المستنصرية /بغداد – العراق

sadeemaaa@yahoo.com

الخلاصة :

تحضير ليكند جديد (4-pentloxy-benzate-salicylidene)-(2-hydroxyl phenyl)-N من تفاعل 4-pentyloxy (4-formyl-3 –hydroxy مع 2-aminophenol بنسب 1:1 ثم تحضير معقداته مع العاصر الانتقالية والتي كان لها الصيغه تم تشخيص اليكندات ومعقداته بواسط تقنية الاشعه تحت الحمراء بالاضافه الى دراسة الكاربون هايدروجين نايتروجين اوكسجين، ودراسة طيف الرنين لمغناطيسي، كما تم التحليل النوعي للمركبات مع التعرف عليها بواسطة تحديد الايون الجزيئي للعينة بواسطة التأين الإلكتروني بواسطه مطياف الكتلة. اثبتت المواد المحضرة ان لها القابلية على تحسس الضوء وتحويله الى تيار كهربائي مما ساعد على استخدام هذه الخاصية في تصنيع خلايا كهربائية من نوع صبغات عضوية حيث كانت نتائج افضل النتائج من الخلايا معقدات النحاس اكثر من خلايا ذات صبغه الليكند.

الكلمات المفتاحية: قواعد شيف – اعناصر انتقالية – صبغات حساسة للخلايا الشمسية – تطبيقات كهروضوئية